

## Inversion studies of magnetic cloud structure at 0.7 AU: Solar cycle variation

T. Mulligan,<sup>1</sup> C. T. Russell,<sup>1</sup> D. Elliott,<sup>1</sup> J. T. Gosling,<sup>2</sup> and J. G. Luhmann<sup>3</sup>

**Abstract.** Pioneer Venus observations from 1979-1988 have revealed the solar cycle evolution of magnetic clouds in the inner heliosphere. Non-force-free magnetic rope models, fit to 44 magnetic clouds, allow us to determine the structures of these clouds and compare their properties with potential field maps of their solar source regions. The leading magnetic polarity in these clouds is correlated with the polarity of the sun's global field. The axis of symmetry of the clouds varies with the inclination of the magnetic streamer belt. At 0.72 AU, the median radius of a magnetic flux rope is 0.10 AU. The median rope contains 11 TWb and carries 0.5 GAmperes of parallel electric current. The occurrence frequency of different handedness of the ropes is equally left and right throughout the solar cycle and shows no correlation with other modeled parameters.

### Introduction

Magnetic clouds are regions of enhanced magnetic fields, within which the solar wind ion temperature is unusually low and the field direction rotates slowly [Burlaga *et al.*, 1981]. They are also a subset of the interplanetary manifestations of coronal mass ejections [Gosling, 1990] comprising about one-third of interplanetary CMEs. They often contain long intervals of strong southward fields and therefore can be a source of intense geomagnetic activity [Burlaga *et al.*, 1990; Lindsay *et al.*, 1995]. Extensive studies of the association of magnetic cloud occurrence and photospheric phenomena such as sigmoidal morphology [Canfield *et al.*, 1999], and X-ray "dimming" associated with a halo coronal mass ejections [Sterling and Hudson, 1997] have helped to bridge the gap between solar observations of CMEs and interplanetary CME (ICME) measurements. Studies by Rust [1994] and Martin and McAllister [1997] have matched magnetic cloud helicities with the helicity of filaments near active regions on the Sun and determined a hemispheric preference for handedness of magnetic clouds. However, Crooker and McAllister [1997] determined that many transients originate in the coronal streamer belt. For clouds borne in this region, such hemispheric helicity arguments are indeterminate. Thus the mechanisms controlling many physical properties of magnetic clouds are still poorly understood.

<sup>1</sup>Institute of Geophysics and Planetary Physics, and the Department of Earth and Space Sciences, University of California Los Angeles

<sup>2</sup>Los Alamos National Laboratory, Los Alamos

<sup>3</sup>Space Sciences Laboratory, University of California Berkeley

Copyright 2001 by the American Geophysical Union.

Paper number 2000GL012016.  
0094-8276/01/2000GL012016\$05.00

Rotations in the field signature of magnetic clouds often seem to be in nearly random directions. However, there was a preference for the magnetic field to rotate from a southward to a northward (SN) orientation during the period 1974-1981 and the opposite sense of this rotation after 1982 [Bothmer and Rust, 1997; Bothmer and Schwenn, 1998; Mulligan *et al.*, 1998]. In all three studies the dominant orientation of the magnetic field in the leading half of these clouds was consistent with the global dipole magnetic field orientation of the Sun.

Since the work of Goldstein [1983], magnetic clouds have been interpreted in terms of magnetic flux ropes [Burlaga, 1988]. The most extensive of these studies have assumed that the flux ropes were force-free cylindrical structures. Mulligan *et al.* [1998] surveyed the Pioneer Venus Orbiter interplanetary data covering over ten years, nearly one full solar cycle, and extending through the solar polarity reversal as mentioned above. They classified magnetic clouds in two categories, as flux ropes with their axes oriented perpendicular to the ecliptic and flux ropes parallel to the ecliptic plane. They named these rope orientations "unipolar" and "bipolar" respectively according to their magnetic signature in the southward component of the field (Bz). It was then possible to follow how the structure of magnetic clouds evolved across the change in polarity of the Sun. However, characterization was performed visually and at best provided only a coarse measure of the orientation of the flux rope axes. Herein we report the first results of a study that extends the prior work of Mulligan *et al.* [1998] by determining quantitatively the orientation, flux content, and twistedness of each rope seen by Pioneer Venus.

### The Inversion technique

Using the downhill-simplex inversion method of Nelder and Mead [1965], a cylindrically symmetric, divergence free magnetic flux rope model using gaussian distributions for magnetic field strengths has been created in order to perform a quantitative analysis of individual flux rope characteristics such as size, orientation, and field strength of observed magnetic clouds. Comparisons of flux rope orientations indicate the model inversions to be consistent with the force-free methods employed by Burlaga *et al.* [1981] and Lepping *et al.* [1990]. The model returns parameters such as axial and poloidal field strengths, cone and clock angles, which serve to determine unambiguously the orientation of the symmetry axis, an impact parameter (i.e., the distance of the closest point of observation to the flux rope axis), radial extent of the rope, and an expansion factor that measures the degree of asymmetry between the leading edge and trailing edge of the rope. The expansion factor  $\delta$  is added to account for field compression observed at the front of many high-speed magnetic clouds and a reduction through the rope due to expansion of the structure as it moves through the heliosphere as reported by Klein and Burlaga [1982]. Other useful char-

acteristics of each rope are determined such as flux content, total current, and degree of twistedness (found by dividing total current by the magnetic flux, analogous to the pitch of the helix). Quantitative simulations by *Cargill et al.* [2000] raise the suggestion that magnetic clouds might be oval in cross section rather than circular. If so, then our quantitative estimates of flux content within the ropes are underestimates but the other parameters, especially orientation, should not be much affected. Figure 1 and Figure 2 show examples of model inversions for two of the flux ropes observed by PVO during late March 1988. The plots are in a coordinate system similar to solar equatorial coordinates, with the positive x-axis pointing anti-sunward and the positive z-axis pointing northward. In both Figure 1 and Figure 2, the flux rope orientation and handedness are shown in the upper corner and the axial field direction is indicated by a thick arrow. In each figure, a field line is drawn so as to be tangent to the axis of the flux rope at its intersection with the ecliptic plane and maps the ends of the flux rope back to its solar source regions. According to *Mulligan et al.* [1998] this line is on average locally aligned along the magnetic neutral line at the Sun.

### Preliminary Results

Figure 3 shows a summary of the flux rope properties at 0.72 AU. Distributions of flux rope size, total flux content, total parallel current, and twistedness are shown over the solar cycle. Of the 44 ropes sampled, 39 are apex crossings. These ropes are such that their axes are oriented roughly perpendicular to the solar direction. Defined in terms of angles, these ropes have cone angles greater than  $35^\circ$  (the cone angle  $\Theta$  is defined such that  $\Theta = 0$  when the axis of the rope is aligned along the solar direction and pointing toward the Sun). The clock angle  $\Phi$ , defined in the plane perpendicular to the radial direction and in a counterclockwise sense with  $0^\circ$  corresponding to the axial field along the northward pointing axis, ranges from  $0^\circ$  to  $360^\circ$  for these ropes. For the other 5 ropes, the spacecraft crosses through a leg of the flux rope, for which the cone angle is less than  $35^\circ$ . This orientation means that the rope axis is quasi-parallel to the solar direction, indicating an extension of the flux rope to-

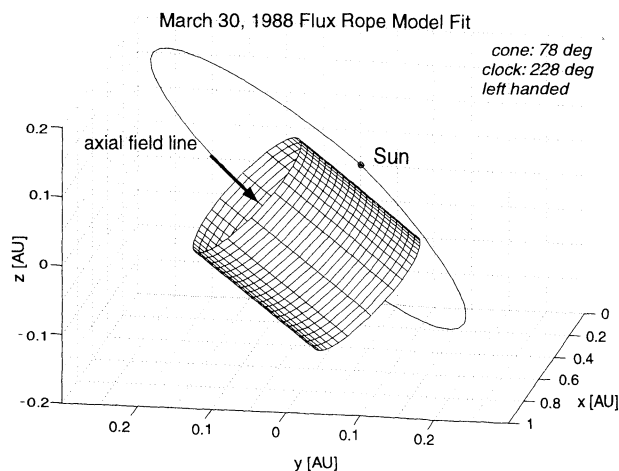


**Figure 1.** 3-D representation of the March 30, 1998 flux rope. The cylinder shows the edges of the flux rope. The field line threads the axis of the cylinder and is tangent to the axial field of the rope at the ecliptic plane.

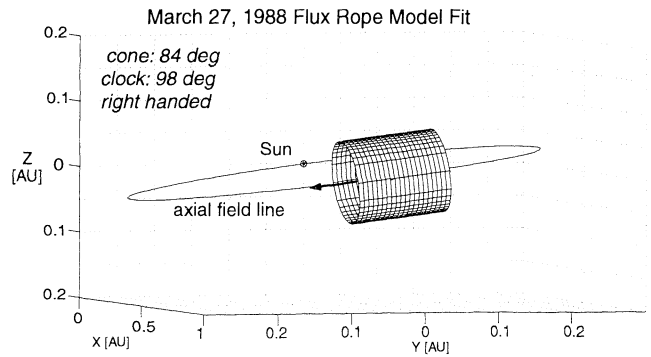


**Figure 2.** 3-D representation of the March 27, 1998 flux rope in the same manner as in Figure 1.

ward the Sun. At the PVO location, modeled rope radii range from approximately 0.04 AU to 0.30 AU with a median radius of about 0.10 AU (0.20 AU diameter). This is consistent with ICME observations at 1 AU [*Klein and Burlaga, 1982; Lepping et al., 1990*]. Total magnetic fluxes of these ropes vary widely from 0.43 TWb ( $4.3 \times 10^{19}$  Mx) to over 100 TWb ( $1.0 \times 10^{22}$  Mx), having a median of 11 TWb ( $1.1 \times 10^{21}$  Mx). Parallel currents derived from  $\nabla \times B$  and integrated over the size of the rope are typically less than 1 GA for the majority of ropes sampled with the median being 0.5 GAmperes. The typical twistedness of these ropes measured in the current per unit of magnetic flux is  $60 \mu\text{Amps per Weber}$  and is equivalent to the force-free parameter ( $\alpha$ ) integrated over the cross sectional area of the rope. Multiplied by  $\mu_0$  the median twist is  $7.5 \times 10^{-11} \text{ m}^{-1}$ . The direction or sign of the twist is an indication of the flux rope handedness. Right-handed ropes are defined as having a positive twist; left-handed ropes have negative twist. The sign of the twist of the modeled ropes is more or less evenly distributed between right and left handed and shows no correlation with other modeled parameters.

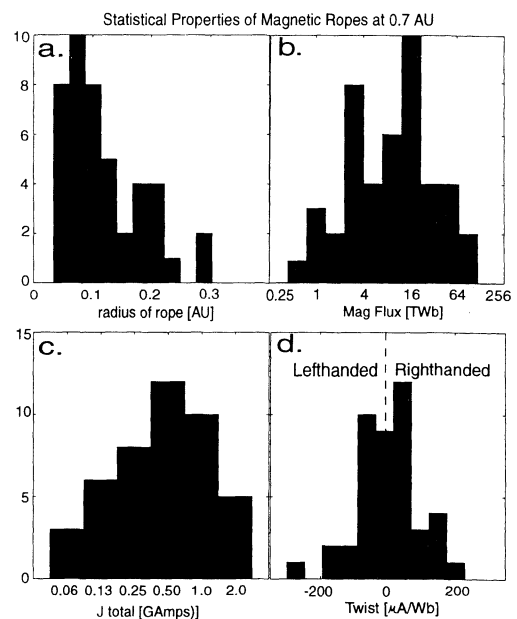


**Figure 3.** Distribution of (a) flux rope radii (b) magnetic fluxes (c) total currents and (d) flux rope twist for the 44 ropes observed in the PVO data.

Although the median magnetic flux reported here is of the same order of magnitude as solar observations of active region magnetic fluxes, the median total current and subsequently the median twist of the modeled ropes is 3 orders smaller than the vertical currents and values of  $\alpha_{AR}$  found in active regions on the Sun [Gary *et al.*, 1987]. Roughly 3/4 of the ropes are well approximated by force-free structures. However, the variation in the amount of twist shown in the bottom right panel appears to be associated with variations in the magnetic forces and amount of expansion in the ropes. Only 9 ropes show no evidence of expansion. The median expansion factor indicates that a typical rope exhibits  $\sim 7\%$  decline in magnetic field strength as the spacecraft traverses the structure.

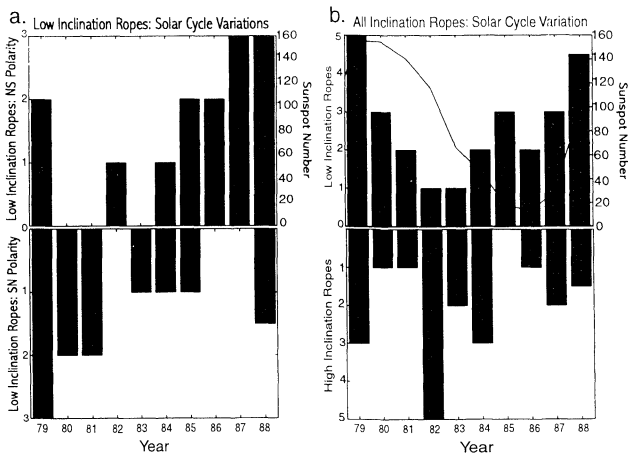
### Solar Cycle Evolution

Mulligan *et al.*, [1998] used visual inspection to characterize the sequence of magnetic field directions in a rope to determine the orientation of magnetic cloud axes. These rope directions were then sorted into four different bins oriented perpendicular to the solar direction. This study improves upon the earlier study with model inversions that provide quantitative flux rope orientations in 3 dimensions, thus allowing us to present the orientations with more confidence and to distinguish crossings of the apex of flux ropes from those of the legs of the structures as defined in the previous section. Figure 4a and Figure 4b show the orientation of the flux ropes over the solar cycle in the same format as in Mulligan *et al.* [1998] but now separated into bins by the direction of the rope axis rather than the sequence of field changes. The top portion of Figure 4a indicates clouds with a north-to-south (NS) rotation in Bz (ropes having clock angles between  $45^\circ$ - $135^\circ$  for right-handed clouds and  $225^\circ$ -

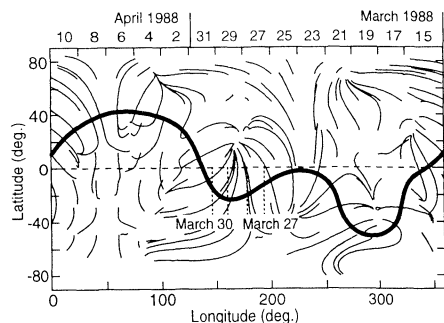
$315^\circ$  for left-handed clouds). The bottom panel shows low inclination ropes with a south-to-north (SN) magnetic signature corresponding to left-handed ropes with axes between  $45^\circ$ - $135^\circ$  and right-handed ropes between  $225^\circ$ - $315^\circ$ . Figure 4 shows that the majority of clouds occurring near the maximum of solar cycle 21 (circa 1979) have SN rotations in their magnetic field vectors while clouds occurring near the maximum of the next solar cycle (circa 1988) have predominantly NS signatures. This suggests the change from predominantly SN to NS rotations in Bz during the declining phase of solar cycle 21 is indicative of a change in polarity of the global magnetic field of the Sun. The distribution of magnetic handedness of these low inclination clouds is equally left and right throughout the study and is not a function of solar cycle. These results are consistent with the visual inspection study of Mulligan *et al.* [1998].

Figure 4a shows that the majority of flux ropes in the low inclination distribution switch leading polarities shortly after the global polar field of the Sun reverses. The solar field reverses polarity approximately at the beginning of 1980. Likewise, the top and bottom panels of Figure 4b show the yearly distribution of low inclination (the ropes from Figure 4a) and high inclination cloud signatures (ropes with clock angles between  $315^\circ$ - $45^\circ$  and  $135^\circ$ - $225^\circ$ ), respectively. Figure 4b indicates that highly inclined cloud orientations are characteristic of the period when the neutral line and streamer belt are also highly inclined just after solar maximum [Behannon *et al.*, 1989; Zhao and Hoeksema, 1996]. The low inclination structures are found from near solar minimum to solar maximum when the streamer belt is more equatorial. As is the case with low inclination clouds, high inclination clouds show little or no preferred magnetic handedness. Thus the occurrence frequency of different handedness of the clouds is not a function of solar cycle. Unlike low inclination clouds, however, highly inclined clouds show no evidence of a preferred leading polarity which reverses when the solar polar field reverses.

Figure 5 shows a Carrington rotation plot of coronal field lines derived from potential field source surface models of Hoeksema and Scherrer [1986] that extend out to at least 2 solar radii ( $R_s$ ). The heavy trace on the source surface is the neutral line, superposed on the field lines to show which arcades form the helmet streamer belt. The highlighted regions of the neutral line indicate the two PVO events shown in Figure 1 and Figure 2. Notice that the orientation of the streamer belt neutral line coincides with the field lines threading the



**Figure 4.** a) (Upper panel) Yearly distribution of low inclination ropes having clock angles between  $45^\circ$ - $135^\circ$  for right-handed clouds and  $225^\circ$ - $315^\circ$  for left-handed clouds. (Lower panel) The distribution of low inclination left-handed flux ropes between  $45^\circ$ - $135^\circ$  and right-handed ropes between  $225^\circ$ - $315^\circ$  over the solar cycle. The two panels indicate a southward leading polarity change to northward leading polarity shortly after solar maximum. Statistics for the last column have been extrapolated through December 1988. (b) (Upper panel) Yearly distributions of the low inclination ropes from Figure 4a and the high inclination flux ropes with clock angles between  $315^\circ$ - $45^\circ$  and  $135^\circ$ - $225^\circ$  (lower panel). The sunspot number is shown for reference in the upper panels.



**Figure 5.** Synoptic plot at  $2R_s$  of coronal field lines from potential field source surface models [Hoeksema and Scherrer, 1986]. The heavy trace is the neutral line to show which arcades form the helmet streamer belt. The dotted regions indicate the two events of Figure 1 and Figure 2.

ropes, which represent the direction of the axial field of the ropes mapped back to the Sun. The time delays corresponding to the differences between Venus and Earth positions relative to the Sun and the convection of the magnetic clouds to Venus have been taken into account in constructing Figures 1 and 2. If we assume the highlighted regions of these figures represent the solar source regions of the magnetic clouds, then we would expect the resulting magnetic cloud structures also to be oriented with their axes as those shown in Figure 1 and Figure 2. This is consistent with our earlier hypothesis that the orientation of the streamer belt controls magnetic cloud orientation.

## Conclusions

This study suggests how the global field of the Sun and the structure of magnetic clouds are intimately linked. Prior studies showed that the leading polarity of clouds whose axes have low inclinations relative to the ecliptic plane, not only reverses when the solar polar field reverses, but also varies in relative frequency over the course of the solar cycle. In contrast, clouds whose axes are highly inclined show no preferred leading polarity and have different solar cycle dependencies than those lying in the ecliptic plane. We have extended the earlier work by applying a non-force-free flux rope model to the observations to include individual flux rope fit comparisons to their presumed solar source regions. The results show a direct correlation between the global polar field and the leading polarity of the magnetic clouds and a direct correlation between the orientation of the streamer belt and the axial orientation of the flux ropes.

These correlations are to be expected if the orientation of magnetic clouds is controlled by the orientation of the streamer belt. The maximum inclination of the streamer belt neutral line, which occurs from just after solar maximum to near solar minimum, produces a large number of clouds highly inclined to the ecliptic plane and is evident in the observations. One can visualize this production in terms of flux rope formation in the highly inclined regions of the streamer belt during the declining phase of the solar cycle. Presuming that the streamer belt is the solar source region of these magnetic clouds is consistent with the association of transients with the streamer belt found by *Crooker and McAllister* [1997] among others.

Distributions of the model parameters indicate the majority of flux ropes have radii that range from approximately 0.04 AU to nearly 0.30 AU. This is consistent with ICME radii observed at 1 AU [*Klein and Burlaga*, 1982; *Lepping et al.*, 1990]. The magnetic ropes in this study have total magnetic fluxes that are comparable to the amount of flux typically found in magnetically active regions on the Sun ( $10 \text{ TWb}$ ,  $10^{21} \text{ Mx}$ ). Total currents are slightly less than 1 GA for the majority of ropes sampled. Handedness of the modeled ropes appears to be equally divided between left and right-handed and shows no obvious correlation with the solar cycle or quantitative flux rope parameters derived from the model. Magnetic fluxes contained within the ropes are of the same order of magnitude as solar observations of active region magnetic fluxes, while total currents and therefore twist of the modeled ropes are approximately 3 orders smaller than the vertical currents and values of  $\alpha_{AR}$  found in active regions on the Sun [*Gary et al.*, 1987]. Variations in the twist in these flux ropes may be associated with the magnetic force balance of the structures. This relationship is currently under investigation.

**Acknowledgments.** This work was supported with a grant from the Institute of Geophysics and Planetary Physics, Los Alamos National Laboratory.

## References

- Behannon, K.W., L.F. Burlaga, J.T. Hoeksema, and L.W. Klein, Spatial variation and evolution of heliospheric sector structure, *J. Geophys. Res.*, *94*, 1245-1260, 1989.
- Bothmer, V., and D. M. Rust, The field configuration of magnetic clouds and the solar cycle, in *Coronal Mass Ejections*, *Geophys. Monogr. Ser.*, vol. 99, edited by N.U. Crooker, J.A. Joselyn, and J. Feynman, p. 139, AGU, Washington, D. C., 1997.
- Bothmer, V., and R. Schwenn, The structure and origin of magnetic clouds in the solar wind, *Ann. Geophys.*, *16*, 1-24, 1998.
- Burlaga, L.F., Magnetic clouds and force-free fields with constant alpha, *J. Geophys. Res.*, *93*, 7217-7224, 1988.
- Burlaga, L.F., E. Sittler, F. Mariani, and R. Schwenn, Magnetic loop behind an interplanetary shock: Voyager, Helios, and IMP 8 Observations, *J. Geophys. Res.*, *86*, 6673-6684, 1981.
- Burlaga, L.F., R.P. Lepping, and J.A. Jones, Global configuration of a magnetic cloud, in *Physics of Magnetic Flux Ropes*, *Geophys. Monogr. Ser.*, vol. 58, edited by C.T. Russell, E.R. Priest, and L.C. Lee, p. 373-377, AGU, Washington, D. C., 1990.
- Canfield, R.C., H.S. Hudson, and D.E. McKenzie, Sigmoidal morphology and eruptive solar activity, *Geophys. Res. Lett.*, *26*, 627-630, 1999.
- Cargill, P.J., J. Schmidt, D.S. Spicer, and S.T. Zalesak, Magnetic structure of overexpanding coronal mass ejections: Numerical models, *J. Geophys. Res.*, *105*, 7509-7519, 2000.
- Crooker, N.U., and A.H. McAllister, Transients associated with recurrent storms, *J. Geophys. Res.*, *102*, 14041-14047, 1997.
- Gary, G.A., R.L. Moore, M.J. Hagyard, and B.M. Haish, Nonpotential features observed in the magnetic field of an active region, *Astrophys. Jour.*, *314*, 782-794, 1987.
- Goldstein, H., On the field configuration of magnetic clouds, in *Solar Wind Five*, edited by M. Neugebauer, *NASA Conf. Publ.* 2280, 731-733, 1983.
- Gosling, J.T., Coronal mass ejections and magnetic flux ropes in interplanetary space, in *Physics of Magnetic Flux Ropes*, *Geophys. Monogr. Ser.*, vol. 58, edited by C.T. Russell, E.R. Priest, and L.C. Lee, pp. 343-364, AGU, Washington, D. C., 1990.
- Hoeksema, J.T. and P.H. Sherrer, Report UAG 94, US Dept. of Commerce, NOAA, Boulder, CO, 1986.
- Klein, L.W., L.F. Burlaga, Interplanetary magnetic clouds at 1 AU, *J. Geophys. Res.*, *87*, 613-624, 1982.
- Lepping, R.P., J.A. Jones, and L.F. Burlaga, Magnetic field structure of interplanetary magnetic clouds at 1 AU, *J. Geophys. Res.*, *95*, 11957-11965, 1990.
- Lindsay, G.M., C.T. Russell, and J.G. Luhmann, Coronal mass ejections and stream interaction region characteristics and their potential geoeffectiveness, *J. Geophys. Res.*, *100*, 16999-17013, 1995.
- Martin, S.F. and A.H. McAllister, Predicting the sign of helicity in erupting filaments and coronal mass ejections, in *Coronal Mass Ejections*, *Geophys. Monogr. Ser. Vol. 99*, edited by N.U. Crooker, J.A. Joselyn, and J. Feynman, pp. 127-138, AGU, Washington D.C., 1997.
- Mulligan, T., C.T. Russell, and J.G. Luhmann, Solar cycle evolution of the structure of magnetic clouds in the inner heliosphere, *Geophys. Res. Lett.*, *25*, 2959-2962, 1998.
- Nelder, J.A., and R. Mead, A simplex method for function minimization, *Computer Journal*, *7*, 308-313, 1965.
- Rust D.M., Spawning and shedding helical magnetic fields in the solar atmosphere, *Geophys. Res. Lett.*, *21* 241-244, 1994.
- Sterling, A.C. and H.S. Hudson, Yohkoh SXT observations of X-ray "dimming" associated with a halo coronal mass ejection, *Astrophys. J. Lett.*, *491*, L55-L58, 1997.
- Zhao, X. and J. T. Hoeksema, Effect of coronal mass ejections on the structure of the heliospheric current sheet, *J. Geophys. Res.*, *101*, 4825-4834, 1996.

T. Mulligan and C. T. Russell, IGPP/UCLA, 405 Hilgard Ave., Los Angeles, CA 90096-1567. (e-mail: tamitha@igpp.ucla.edu; crussell@igpp.ucla.edu)

(Received July 6, 2000; revised October 20, 2000; accepted October 26, 2000.)